AE 403, Dr. Attia

Preliminary Design of a HPT Stage

Embry-Riddle Aeronautical University

Matthew Liepke
4-20-2021

Executive Summary

Enclosed in this report is a proposal for the first axial turbine stage to a high-bypass turbofan engine that produces 28.45 MW, operating at 12,0000 rpm. This proposed stage has a near linear axial velocity climb rate below 10% across all blades. The mid radius of the annulus decreases as flow progresses through the turbine by less than 3% across each geometric station, designed to maintain a constant tip radius along the annulus. The flow exiting the stage has slight swirl, with an α_3 of 12.03 degrees. All internal turn angles fall within general guidance; the maximum turn angle the flow experiences is 107 degrees at the rotor's hub. For initial design of blades using a Zweifel coefficient of 0.8 for both rotor and stator, the proposed stage has 59 stator blades and 100 rotor blades. The reaction at the rotor hub is 9.620%, with a maximum mid-radius Mach of 1.297 at the station between the stator and rotor.

Table 1: Design Choices

	Units	Value	Notes
RPM	rpm	12000.0000	
Zweifel (mid)	(--)	0.8000	
Φ	(--)	0.8000	
Vax 1 --> 2	%	109.3765	Vax1 to Vax2 in % of Vax1
Vax 2 --> 3	%	108.3996	Vax2 to Vax3 in % of Vax2
rm 2 --> 3	%	0.9830	rm2 to rm3 in % of rm2
rm 1 --> 2	%	0.9742	rm1 to rm2 in % of rm1
α_3	deg	12.0294	
Rotor Aspect Ratio	(--)	1.0500	
Rotor Taper Ratio	(--)	0.8700	
Stator Aspect Ratio	(--)	0.8000	
Stator Taper Ratio	(--)	1.2000	

Table 2: Major Stage Characteristics

	Units	Value
Power Produced	MW	28.4469
Hub Reaction	%	9.6199
λ	(--)	2.0190
Maximum Mid Radius Mach	(--)	1.2972
Maximum Turn Angle	deg	106.952
Stator Blade Count	(--)	59.0000
Rotor Blade Count	(--)	100.0000

Table of Contents

List of Figures

List of Tables

Introduction

The design of the proposed stage was completed using general guidance from Attia's *Axial Turbine Lectures* and Farhokhi's *Aircraft Propulsion* textbook. (Attia) (Farokhi) The process of calculating the properties and performance of the stage nearly directly followed Attia's Lecture 4, with slight modifications done in order to vectorize calculations. This vectorization was done so MATLAB's Parallel Computing Toolbox[1] could be used to produce a range of valid design choices that met all criteria specified for the engineer to choose from. The criteria specified are shown below in Table 3 and were given to the engineer as hard requirements to meet for the stage design. All values were validated after the original design to ensure the proposed design met the specified requirements.

Table 3: Specified State Requirement Constraints

	Units	Value
$\dot{m}$	$kg\ s^{-1}$	70.000
η_{tt}	(--)	0.910
T_{0_1}	K	1700.000
p_o	Pa	2050e+03
M_1	(--)	0.400
$\dfrac{p_{0_1}}{p_{0_3}}$	(--)	3.200
ξ_s	(--)	0.053

Convention

All images herein demonstrate a clockwise-rotating turbine stage. All angles provided are assumed to be positive if they follow the traditional flow paths shown in Figure 1. All units described are in SI with degrees and will be indicated in the 'Units' column of the given table where the values are found. Conditions referenced follow the convention in Figure 1, with the process between station $(1) \rightarrow (2)$ being that of the stator, and between station $(2) \rightarrow (3)$ being that of the rotor. A subscript 'r' was used for the rotor-relative frame of reference, where total conditions change to describe the flow as the rotor sees it.
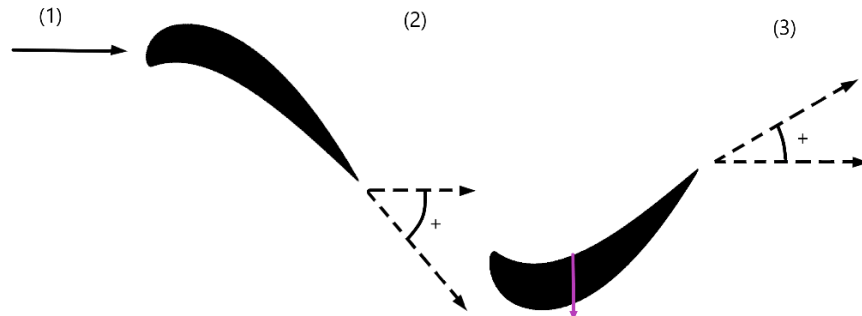

Figure 1: Angle & Station Convention Used for a Clockwise Stage

Results

For axial flow paths, the predominant feature in the proposed annulus is the constant tip radius, designed to reduce the centrifugal stresses on the blade and allow for better mixing of bypass gases downstream (Farokhi 693). This was accomplished by iteratively changing the mid radius to accommodate this design constraint chosen by the engineer. The final meridional view of the stage can be seen below, in Figure 2, with tables regarding the positioning found in Table 4.

---

1 MATLAB Parallel Computing Toolbox Release 2021a, The MathWorks, Inc., Natick, Massachusetts, United States
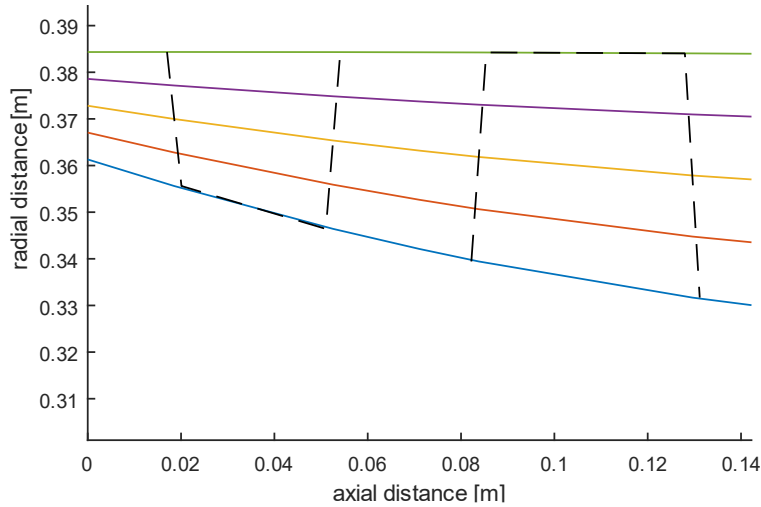
Figure 2: Meridional View of Stage with Rotor and Stator Blade Outlines

Table 4: Complete Meridional Spacing Information

	Units	Cond. 1	Stator LE	Stator TE	Cond. 2	Rotor LE	Rotor TE	Cond. 3
A	m^2	0.0540	0.0668	0.0870	0.0963	0.1019	0.1177	0.1209
r_t	m	0.3843	0.3843	0.3843	0.3843	0.3843	0.3840	0.3840
r_m	m	0.3728	0.3700	0.3654	0.3632	0.3618	0.3579	0.3570
r_h	m	0.3613	0.3556	0.3464	0.3421	0.3394	0.3317	0.3301
x_m	m	0.0000	0.0185	0.0526	0.0711	0.0838	0.1296	0.1422

For the design of the blades, the stagger caused by the Free-Vortex solution was low for the rotor, a side-effect of the low hub reaction constraint given. The stator does experience some variance in its stagger, although the design is still well in the range of possible manufacturing.
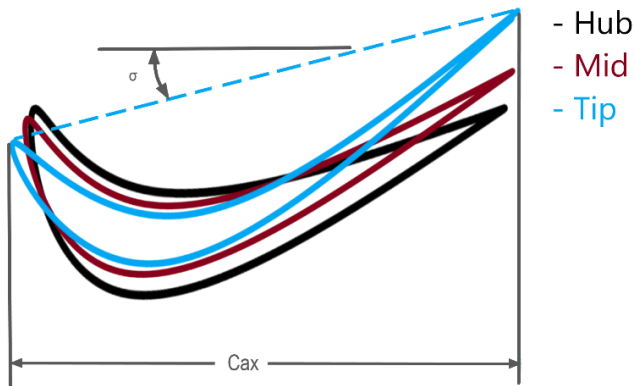

- Hub
- Mid
- Tip

Figure 3: Rotor Stagger

Table 5: Blade Characteristics

	Units	Stator	Rotor
$c_{ax,h}$	m	0.0371	0.0489
c_{ax}	m	0.0340	0.0458
$c_{ax,t}$	m	0.0309	0.0426
c_h	m	0.0451	0.0489
c_m	m	0.0410	0.0459
c_t	m	0.0371	0.0430
σ_h	deg	34.5325	0.7157
σ_m	deg	33.9477	4.1737
σ_t	deg	33.3725	8.0349

For thermodynamic properties including Mollier diagrams and velocity triangle solutions at the hub, mid and tip, see the Appendices. Charts and diagrams for the complete thermodynamic properties of the stage can be found in Appendix I – Mollier Diagrams, and tables for velocity triangle solutions for the mid, hub and tip at each station can be found in Appendix 2 – Velocity Triangle Tables for Mid, Hub and Tip.

Computational Method

To produce a desirable stage, many stages were tested in quick concession with MATLAB, automatically varying design parameters such as Φ, λ, α_2, and V_{ax2}. The information provided from these tests proved to be a tremendous aid in the design process, as they allowed for a better understanding of the impact each design choice had on the final product. In the figures below a scatter plot of Φ, λ, and α_2 can be found, where each point

represents a potential stage that meets all design criteria and general rules of thumb. This means for each point the hub reaction was $10\% \pm 1\%$, the maximum mid-radius Mach did not exceed 1.3, the difference between the number of stator and rotor blades was greater than four, α_2 was limited to below 72 degrees, and the maximum turn angle for the rotor did not exceed 120 degrees. It is important to note that for both figures some design choices were held constant; they may be used to make generalization for turbine stages, but specific values may not be applicable to all turbine stages.
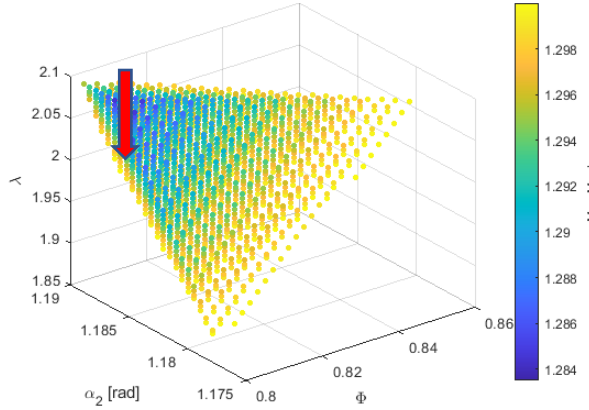

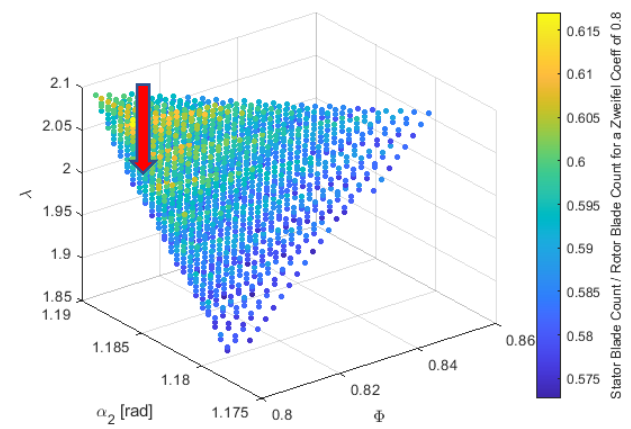Figure 4: Mach Scatter Plot with Current Stage in Red

Figure 5: Blade Ratio Scatter Plot with Current Stage in Red

Using Figure 4 to limit the maximum Mach in the stage, the work coefficient λ must be set to a relatively high value, with an α_2 at the higher range of solutions and a low Φ. In Figure 5 the same trend was determined to benefit the ratio of stators and rotors, assuming a ratio of 2:3 is desired (Attia). Figures such as these were used in conjunction with an auto-generated meridional view to intelligently optimize the stage without guesswork.

From figures such as Figure 4 and Figure 5 the design choices indicated in Table 1 in the Executive Summary were selected. It was chosen to pick values of as λ, α_2, and V_{ax2} that were not at along the edges of the solution set, rather towards the center of the solution set in the upper left of the figures shown. This was done so that no design parameters were at extremes, with the thought that operating at the limit of constraints could lead to a decreased product lifespan.

Procedure Followed

For the thermodynamic properties of the stage, each test started by finding p_1 and T_1 using the isentropic relations with the pre-defined M_1 design constraint. Also calculated was V_{ax1} via the speed of sound definition. Since the flow is assumed axial, $V_{u1} = 0$ and thus the inlet velocity triangle was known. Then, p_{0_2} was calculated via ξ_s using Eq. 4.

$$p_{0_1} = p_1 \left(1 + \frac{\gamma - 1}{2} M_1^2\right)^{\frac{\gamma}{\gamma - 1}}$$

Eq. 1

$$T_{0_1} = T_1(1 + \frac{\gamma - 1}{2} M_1^2)$$

Eq. 2

$$V_{ax1} = M_1\sqrt{\gamma R \, T_1}$$

Eq. 3

$$\xi_x = \frac{p_{0_1} - p_{0_2}}{\frac{1}{2}\rho_1 |V_1|^2}$$

Eq. 4

Turning to rotor thermodynamics, p_{0_3} was found using the stage total pressure ratio, which makes way for T_{0_3} to be calculated using η_{tt}. With all total temperatures defined, the total enthalpy change across the stage was extracted under the assumption that Cp does not vary in the flow. This, in combination with the $\dot{m}$ constraint of the stage provides the work the stage is expected to extract, not taking mechanical losses into account.

$$p_{0_3} = \frac{p_{0_3}}{p_{0_1}} p_{0_1}$$

Eq. 5

$$\eta_{tt} = \frac{1 - \left(\frac{T_{0_3}}{T_{0_1}}\right)}{1 - \left(\frac{p_{0_3}}{p_{0_1}}\right)^{\frac{\gamma-1}{\gamma}}}$$

Eq. 6

$$\Delta h_0 = C_p(T_{0_1} - T_{0_3})$$

Eq. 7

$$P = \Delta h_0 \dot{m}$$

Eq. 8

Now λ, Φ, r_{m1}, r_{m2}, V_{ax2}, and α_2 were input into the simulation as design choices. These were used to start to bridge the gap to geometry, using Eq. 9 and Eq. 10. With U_3 available, the mid exit radius of station 3 was determined using Eq. 11. With that calculated, the mid radius at station 1 was used to calculate U_2. The rotor inlet triangle was completed using V_{ax2} and α_2, which allowed the calculation of V_{u2} using trigonometry.

$$U_3 = \sqrt{\frac{\Delta h_0}{\lambda}}$$

Eq. 9

$$V_{ax3} = \Phi U_3$$

Eq. 10

$$r_{m3} = \frac{U_3}{\omega}$$

Eq. 11

$$V_{u2} = V_{ax2} \tan(\alpha_2)$$

Eq. 12

$$U_2 = \omega r_{m2}$$

Eq. 13

With values for U_2, U_3, V_{ax2}, V_{ax3}, and V_{u2}, only one more component of the rotor's velocity triangle was required to complete it. It was chosen to use the Euler Turbomachinery Equation at the mid-radius in Eq. 14 to find V_{u3}. Here it was important to check the sign of V_{u3}; any negative values for V_{u3} were flagged and filtered out for unconventional triangles in MATLAB. Once Eq. 15 was performed, trigonometry was used to complete the rest of the velocity triangles, using Figure 10 as a reference. These values can be found in Appendix 2 – Velocity Triangle Tables for Mid, Hub and Tip

$$\Delta h_0 = U_3 V_{u3} + U_2 V_{u2}$$

Eq. 14

$$U_2 = \omega r_{m2}$$

Eq. 15

With velocity triangles complete, the annulus shape became the next step in the design. Eq. 16, Eq. 17, Eq. 18 and Eq. 19 were performed to calculate A_2 and A_3, while calculation of A_1 only required Eq. 19. The tip and hub radius at each station were then found using a system of equations containing the mid radius definition and the area equation for an annulus. At this point in the procedure, all thermodynamic properties were known. The Mollier Diagrams and accompanying information for each component and the combined stage are found in Appendix I – Mollier Diagrams.

$$T = T_0 - \frac{1}{2Cp}|V|^2$$

Eq. 16

$$M = \frac{|V|}{\sqrt{\gamma RT}}$$

Eq. 17

$$p_0 = p_1 \left(1 + \frac{\gamma - 1}{2} M^2\right)^{\frac{\gamma}{\gamma-1}}$$

Eq. 18

$$A = \frac{\dot{m}RT}{|V|^2 p}$$

Eq. 19

$$A = \pi(r_t^2 - r_h^2)$$

Eq. 20

$$r_m = \frac{r_t + r_h}{2}$$

Eq. 21

Now that all radii at stations were known, arrays representing the radii were created using the hub and tip radii, spaced so that any number of flow paths could be solved for. Afterwards, the velocity triangles were modified using the Free-Vortex Solution shown in Eq. 22 and Eq. 23, with the assumption that V_{ax} did not change with respect to radius. The rest of the values for the velocity triangles were calculated referencing Figure 10, and the results for the designed stage are shown in Appendix 2 – Velocity Triangle Tables for Mid, Hub and Tip.

$$V_u(r) = \frac{r_m}{r} V_{um} \qquad \text{Eq. 22}$$

$$U(r) = \omega r \qquad \text{Eq. 23}$$

With the velocity triangles the blades must produce established, their shapes were developed. Using Eq. 24 to find the stagger for the stator and rotor blades, and Eq. 25 through Eq. 27 to find the rest of the properties of the blades, the rotor could be visualized in Figure 3, found at the beginning of the Results section. The proposed stage does not have very high change in stagger from hub to tip, caused by the low radius ratio stage components.

$$\sigma_s = \frac{\beta_2 + \beta_3}{2} = \frac{\alpha_1 + \alpha_2 2}{2} \qquad \text{Eq. 24}$$

$$b_{avg} = \overline{r_t} - \overline{r_h} \qquad \text{Eq. 25}$$

$$Taper\ Ratio = \frac{c_{ax,t}}{c_{ax,h}} \qquad \text{Eq. 26}$$

$$c_{ax} = c_m \cos(\sigma_s) \qquad \text{Eq. 27}$$

One of the last things that needed to be designed was the meridional view. Using a spacing of 2.8" between the center of the rotor and stator, which provided similar spacing to method recommended in *Axial Turbines Lecture 4* (Attia), the axial distance from the combustion chamber exit was calculated for the mid radius of station (2) and (3). Afterwards, second order polynomials were used to create the annulus shape, using the radii at station (1), (2), and (3) as the constraint points. Points for the leading edge and trailing edge of each blade then were interpolated, shown in Figure 2 at the beginning of the Results section. In the figure shown five polynomials were solved for, producing five different colored meridional flow paths. Information regarding the axial positioning and radial distances can be found in Table 4, alongside Figure 2 at the beginning of the Results section.

Finally, the number of blades to be recommended was calculated using zweifel's coefficient. Since this is a heavily loaded HPT stage with further design such as material selection needing to be finalized, it was chosen to pick a zweifel coeficcient of .8, which was determined as it was what Zweifel recommended, according to *Aircraft Propulsion* (Farokhi 716). These equations resulted in 59 stator blades and 100 rotor blades, shown in Table 2 in the Executive Summary.

$$\psi_z = \frac{2s}{c_{ax}} \cos^2 \beta_3 (\tan \beta_2 - \tan \beta_3) = \frac{2s}{c_{ax}} \cos^2 \beta_3 (\tan \beta_2 - \tan \beta_3) \qquad \text{Eq. 28}$$

$$blade\ count = \frac{2\pi r}{s} \qquad \text{Eq. 29}$$

Design Validation

As a final design verification to ensure that the proposed stage is reasonable, the characteristics of the stage were plotted on a Smith Chart with other designs. Seen as the red dot, the proposed stage falls closely in line with the contours of η_{tt} that the stage was designed for. This is a generic indication that the proposed stage may very well align with other designs, meaning it is feasible.
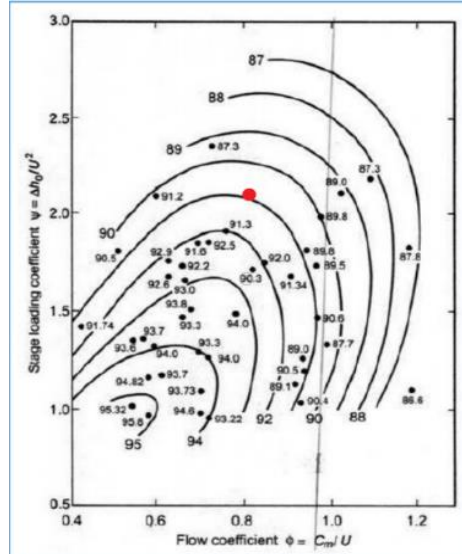

Figure 6: Smith Chart with Proposed Stage Marked in Red. Source: (Hany Moustapha)

References

Attia, Madgy. *AE 403: Axial Turbines - Lecture 1-4*. 2021. PDF Notes.

Farokhi, Saeed. *Aircraft Propulsion*. Second. John Wiley & Sons Ltd, 2014.

Hany Moustapha, Mark F. Zelesky, N.C.B and Japikse, D. *Axial and Radiual Turbines*. Concepts ETI, 2003.
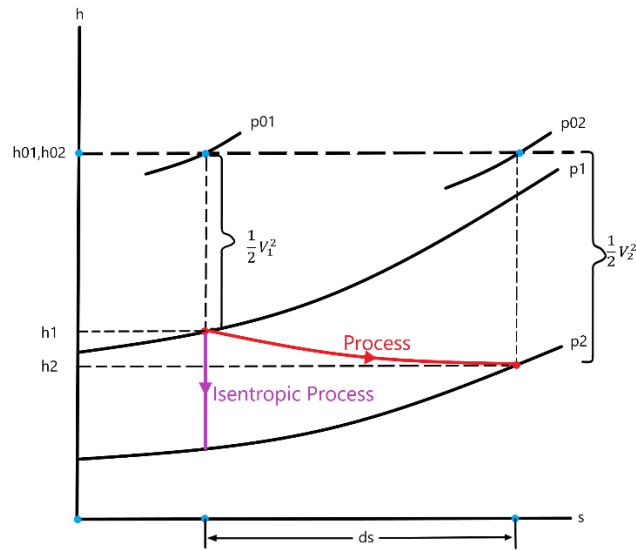
Appendix I – Mollier Diagrams

Figure 7: Mollier Diagram for Stator
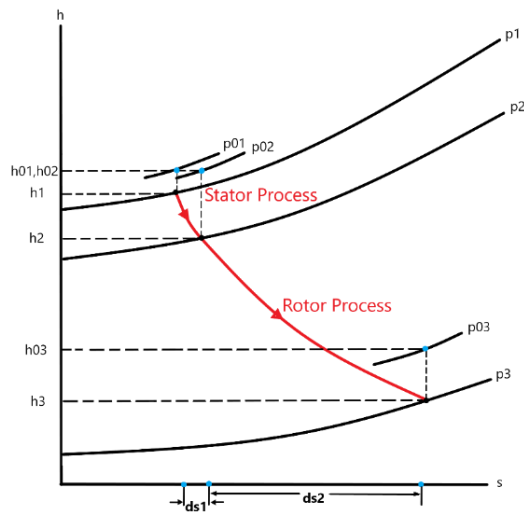
Figure 8: Mollier Diagram for Complete Stage

Table 6: Complete Absolute Thermodynamic Conditions

	Units	Condition 1:	Condition 2:	Condition 3:
h_0	$J\ kg^{-1}$	1.7814e+06	1.7814e+06	1.3750e+06
h	$J\ kg^{-1}$	1.7356e+06	1.3943e+06	1.3078e+06
M	(--)	0.4000	1.2972	0.5586
p_o	Pa	2.0500e+06	2.0396e+06	6.4063e+05
p	Pa	1.8456e+06	7.5977e+05	5.2353e+05
Δs	$J\ kg^{-1}K^{-1}$	1.3234		29.763
T_o	K	1700	1700	1312.2
T	K	1656.3	1330.6	1248.1
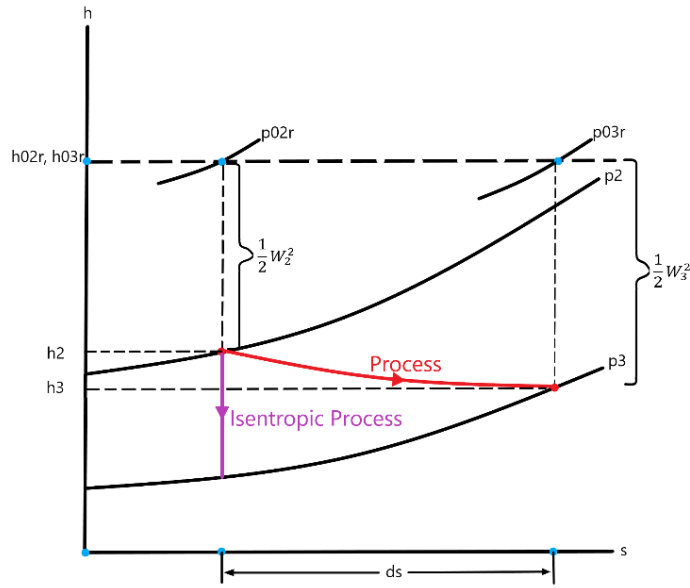
Figure 9: Mollier Diagram for Rotor in the Relative Frame

Table 7: Rotor Relative Thermodynamic Conditions

	Units	Condition 1:	Condition 2:
h_{0_r}	$J\,kg^{-1}$	1.5130e+06	1.5100e+06
h	$J\,kg^{-1}$	1.3943e+06	1.3078e+06
M_r	(--)	0.7185	0.9654
p_{o_r}	Pa	1.0562e+06	9.3182e+05
p	Pa	7.5977e+05	5.2353e+05
T_{o_r}	K	1444.3	1441.0
T	K	1330.6	1248.1
Δs	$J\,kg^{-1}K^{-1}$		29.763

Appendix 2 – Velocity Triangle Tables for Mid, Hub and Tip
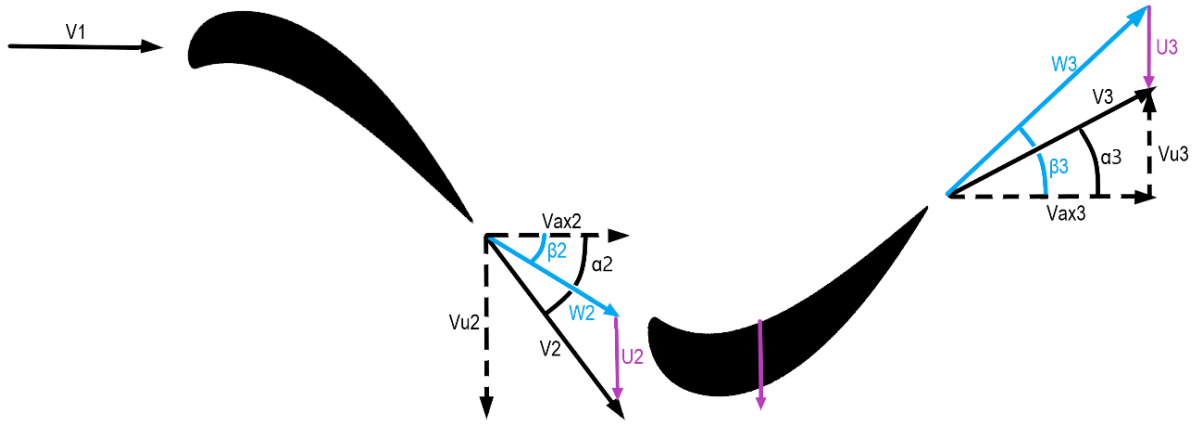
Figure 10: Velocity Triangles for Stage

Table 8: Stator Inlet Velocity Triangle Table – Condition 1

	Units	Hub	Mid	Tip
α	deg	0.000	0.000	0.000
β	deg	0.000	0.000	0.000
U	$m\,s^{-1}$	0.000	0.000	0.000
V_{ax}	$m\,s^{-1}$	302.718	302.718	302.718
V_u	$m\,s^{-1}$	0.000	0.000	0.000
$|V|$	$m\,s^{-1}$	302.718	302.718	302.718
W_{ax}	$m\,s^{-1}$	0.000	0.000	0.000
W_u	$m\,s^{-1}$	0.000	0.000	0.000
$|W|$	$m\,s^{-1}$	0.000	0.000	0.000

Table 9: Stator Exit / Rotor Inlet Velocity Triangle Table – Condition 2

	Units	Hub	Mid	Tip
α	deg	69.065	67.895	66.745
β	deg	52.760	47.301	40.975
U	$m\,s^{-1}$	429.899	456.404	482.909
V_{ax}	$m\,s^{-1}$	331.103	331.103	331.103
V_u	$m\,s^{-1}$	865.485	815.224	770.480
$|V|$	$m\,s^{-1}$	926.657	879.897	838.611
W_{ax}	$m\,s^{-1}$	331.103	331.103	331.103
W_u	$m\,s^{-1}$	435.586	358.820	287.571
$|W|$	$m\,s^{-1}$	547.142	488.242	438.550

Table 10: Rotor Exit Velocity Triangle Table – Condition 3

	Units	Hub	Mid	Tip
α	deg	12.980	12.029	11.207
β	deg	54.192	55.648	57.045
U	$m\,s^{-1}$	414.769	448.642	482.516
V_{ax}	$m\,s^{-1}$	358.914	358.914	358.914
V_u	$m\,s^{-1}$	82.728	76.482	71.113
$|V|$	$m\,s^{-1}$	368.325	366.972	365.891
W_{ax}	$m\,s^{-1}$	358.914	358.914	358.914
W_u	$m\,s^{-1}$	497.497	525.124	553.628
$|W|$	$m\,s^{-1}$	613.451	636.062	659.791